Thermal and calorific effects accompanying the stress softening

Jose Ricardo Samaca Martinez, Jean-Benoit Le Cam, Xavier Balandraud, Evelyne Toussaint, J Caillard

Thermal and calorific effects accompanying the stress softening

J.R. Samaca Martinez
Clermont Université, Institut Français de Mécanique Avancée, Université Blaise Pascal, Institut Pascal, CNRS, UMR 6602, Clermont-Ferrand, France
Michelin, CERL Ladoux, Clermont-Ferrand, France

J.-B. Le Cam
Institut de Physique de Rennes, UMR 6251, Université De Rennes 1, Rennes, France

X. Balandraud & E. Toussaint
Clermont Université, Institut Français de Mécanique Avancée, Université Blaise Pascal, Institut Pascal, CNRS, UMR 6602, Clermont-Ferrand, France

J. Caillard
Michelin, CERL Ladoux, Clermont-Ferrand, France

ABSTRACT: This study investigates thermomechanical effects in filled rubbers under cyclic uniaxial tensile loading at ambient temperature. More especially, it focuses on the calorific response of crystallizing (NR) and non-crystallizing (SBR) rubbers during stress softening, which occurs during the first mechanical cycles. Temperature changes were measured by infrared thermography. Heat sources produced or absorbed by the material due to deformation processes were deduced from these temperature changes by using the heat equation. Heat source variations during each mechanical cycle were analysed and the mechanical dissipation produced in each cycle was deduced. For both materials, the relative contribution to mechanical dissipation of dissipative mechanisms involved in stress softening and viscosity was determined.

1 INTRODUCTION

One of the main phenomena in the mechanics of rubber-like materials dates from the observation by Bouasse & Carrière in 1903 (Bouasse & Carrière 1903) of stress softening after the first mechanical load. Later, this phenomenon was studied more precisely by Mullins in 1948 (Mullins 1948) and was then referred to as "the Mullins effect".

Despite the numerous studies reported in the literature since the work of these pioneers, no consensus has been found on the physical origin of the Mullins effect. Among the phenomena described, one can cite bond rupture (Blanchard & Parkinson 1952), chain rupture (Bueche 1960), chain slipping (Houwink 1956), chain disentanglement (Hamed & Hatfield 1989), filler-cluster breakdown (Kraus et al. 1966, Kluppel & Schramm 2000) and network rearrangement (Marckmann et al. 2002, Diani et al. 2006). The most recent study in this field incriminates a layer of polymer whose movements are hindered (Diaz et al. 2014). According to the authors, this layer adds to the filler reinforcement and its desorption creates Mullins softening. Up to now, the Mullins effect has only been investigated from a mechanical point of view, while its thermal and calorimetric signatures might provide information of paramount importance. In this study, we propose to measure the temperature changes during the deformation of rubbers by using Infrared Thermography (IRT). It can be noted that in the tests performed in the present study, stress softening in rubbers is accompanied by heat production and heat exchanges with the outside. Moreover, during the first cycles, the temperature evolution is not stabilized. Consequently, the analysis of the temperature does not provide a clear understanding of the thermomechanical phenomena. For this reason, temperature variation cannot easily be used to study the thermal effects accompanying stress softening. This is the reason why we use the framework of the Thermodynamics of Irreversible Processes (TIP) and the heat diffusion equation to measure the total heat source produced or absorbed by the material. This approach is applied in the present study in order to identify the calorimetric signature of the Mullins effect, *i.e.* the mechanical dissipation due to stress softening.

2 EXPERIMENTAL SETUP

2.1 *Materials and specimen geometry*

The materials considered here were Natural Rubber (NR) and Styrene-Butadiene Rubber (SBR), both filled with the same amount of carbon black 50 part per hundred of rubber in weight (phr). They are respectively denoted NR50 and SBR50 in the following. Apart from the macromolecules themselves, the compounds had the same chemical composition. It should be noted that only the NR50 formulation is subject to stress-induced crystallization: the characteristic stretch ratios at which crystallization and crystallite melting occur are denoted by λ_c and λ_m and are close to 1.8 and 1.6, respectively. Thin dumbbell-shaped specimens were used. They were 5 mm in width, 10 mm in length and 1.4 mm in thickness.

2.2 *Loading conditions*

The mechanical tests corresponded to cyclic uniaxial tensile loadings. They were applied under prescribed displacement using an INSTRON 5543 testing machine with a load cell capacity of 500 N. The signal shape was triangular in order to ensure a constant strain rate during loading and unloading. The loading rate and the nominal strain rate $\dot{\lambda}$ were equal to ±300 mm/min and ±0.5 s^{-1}, respectively. The tests corresponded to 4 series composed of uniaxial mechanical cycles, at four different maximum stretch ratios. The number of cycles for each maximum stretch ratio was chosen in such a way that the mechanical response was stabilized for the last cycle. This number was equal to 5 for NR50 and 3 for SBR50. The following maximum stretch ratios were chosen (see Fig. 1):

– for NR50, the four maximum stretch ratios denoted by λ_1, λ_2, λ_3, λ_4 were chosen equal to 1.4, 2, 4 and 6, respectively. λ_1 was chosen as lower than λ_c. λ_2 was close to λ_c. λ_3 and λ_4 were higher than λ_c (λ_4 was close to the failure stretch ratio).
– for SBR50, the four maximum stretch ratios λ_1, λ_2, λ_3, λ_4 were chosen equal to 2, 3, 4 and 4.5, respectively.

Temperature field measurements were performed using a Cedip Jade III-MWIR infrared camera. The thermal quantity extracted from the measurement was the mean temperature change over a small zone of 5 × 5 px (1 mm^2) at the centre of the specimen.

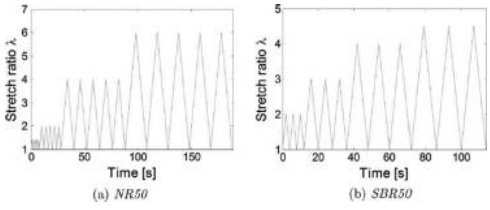

Figure 1. Mechanical loading conditions.

2.3 *Brief reminder of heat source calculation*

It is now well known that temperature is not the most relevant quantity to consider in the study of phenomena involved during the deformation of material. Indeed, stress softening can be accompanied by heat exchanges with the specimen outside (non-adiabaticity of the thermomechanical evolution). For this reason, temperature variation cannot be used to study the calorific phenomena accompanying stress softening. Temperature is the consequence of the heat produced or absorbed by the material due to stretching, but also of the heat diffusion in the specimen and of the heat exchanges with the outside. Assuming that the heat source fields are homogeneous in the specimen, the heat diffusion equation can be written in a '0D' formulation as follows (Chrysochoos 1995):

$$\rho C_{E,V_k}\left(\dot{\theta}+\frac{\theta}{\tau}\right)=s \tag{1}$$

where ρ is the density, C_{E,V_k} is the specific heat at constant E and V_k (state variables), θ is the difference between the current and the initial temperature of the material, τ is a time constant characterizing the heat exchanges between the specimen and its environment, *i.e.* the ambient air and the jaws of the testing machine.

In practice, the constant τ is experimentally assessed by identification from a simple test of natural return to room temperature. It can be noted that τ must be measured for each testing configuration (material, specimen geometry, stretch applied, environment in terms of ambient air and jaws of the testing machine). In the present case, a linear expression of τ as a function of the stretch ratio λ has been experimentally determined (Samaca Martinez et al. 2013b, Samaca Martinez et al. 2013c):

$$\tau(\lambda)=40.48-3.25\lambda \tag{2}$$

It should be noted that the function used was the same whatever the material considered because the product of the density by the heat capacity does not change from one compound to another, the initial thickness being the same. The right-hand side of equation (1) represents the total heat source s produced by the material itself. It can be divided into two terms:

– *mechanical dissipation* d_1 *(intrinsic dissipation):* this positive quantity corresponds to the heat

source which is produced due to mechanical irreversibilities;
– *thermomechanical coupling heat sources*: these correspond to the couplings between the temperature and the other state variables.

The heat source s is expressed in $W \cdot m^{-3}$. However, it is generally useful to divide this quantity by $\rho C_{E,V_k}$, so hat equation (1) writes:

$$\dot{\theta} + \frac{\theta}{\tau} = \frac{s}{\rho C_{E,V_k}} \tag{3}$$

The quantity $s/\rho C_{E,V_k}$ is expressed in °C/s. It corresponds to the temperature rate that would be obtained in an adiabatic case, *i.e.* for an infinite value of τ. In the rest of this paper, the term "heat source" will also be used for this quantity $s/\rho C_{E,V_k}$.

3 RESULTS

3.1 *Mechanical response*

The mechanical responses obtained for NR50 and SBR50 are presented in Figure 2a and 2b, respectively.

The following comments can be made:

– most of the softening was obtained after the first load of the series, whatever the maximum stretch ratio applied. The maximum nominal stress considerably decreased between the two first cycles, approximately 30% for NR50 and 12% for SBR50. These values have been calculated using the maximum stress during cycle 1 et 2 for the two last series of cycles (for λ_3 and λ_4);

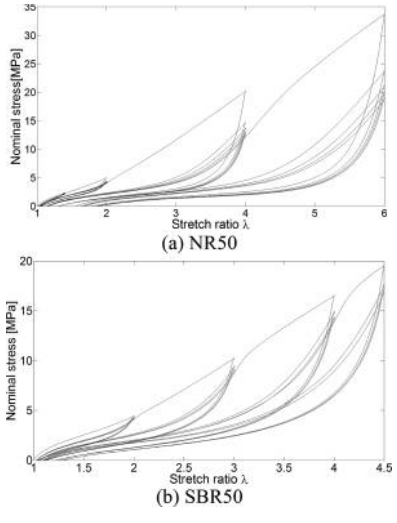

Figure 2. Mechanical cycles for four increasing maximum stretch ratios.

– a hysteresis loop was observed for both filled materials. The mechanical response of NR50 exhibited a larger hysteresis loop;
– a residual strain was observed. It reached 80% and 35% at the end of the test for NR50 and SBR50, respectively;
– when the stretch ratio exceeded the maximum stretch ratio previously applied, the gap (in terms of the stretch ratio) to return to the maximum stress previously obtained was larger for NR50. It should be recalled that, compared to SBR50, NR50 exhibited a higher residual strain. Moreover, the curve of the first load, obtained for higher maximum stretch ratios, did not join what would be the monotonous tensile curve.

3.2 *Calorimetric response in filled non crystallizable rubbers (SBR50)*

In this section, heat sources obtained with SBR50 are analyzed qualitatively for each series of maximum stretch ratios applied.

Series #1 (three cycles at $\lambda_1 = 2$), Figure 3(a): during the loading phases, the heat source was positive and increased with the stretch ratio. The heat sources produced during the first loading were slightly larger than those produced during the two following loadings. The heat sources produced during loading were stabilized from the second cycle (similar evolution during the second and third loading phases). During the three unloading phases, the heat sources were negative (heat absorbed by the material). The three curves can nearly be superimposed, meaning that the number of mechanical cycles had no significant effect on the deformation processes during unloading. Consequently, this highlights that a larger mechanical dissipation was produced during the first cycle: this can be seen as damage associated with stress softening. This is in good agreement with the fact that a larger hysteresis loop was observed for the first cycle in the mechanical response;

Series #2 (three cycles at $\lambda_2 = 3$), Figure 3(b): during the loading phases, when the stretch ratio exceeded the maximum stretch ratio previously applied (in this case $\lambda = 2$), a high increase in heat source production was observed. This result strongly echoes that obtained with the mechanical response. From the third cycle, the heat sources produced during the loading phases evolved similarly during the following cycles (not reported here), meaning that the calorimetric signature of the Mullins effect is mainly observed between the first and second loads. As previously observed for the lowest maximum stretch ratio (λ_1), the curves can be superimposed during the unloading phases;

Series #3 (three cycles at $\lambda_3 = 4$), Figure 3(c): results are similar to the previous ones: when the stretch ratio exceeded the maximum stretch ratio previously applied (in this case $\lambda = 3$), a high

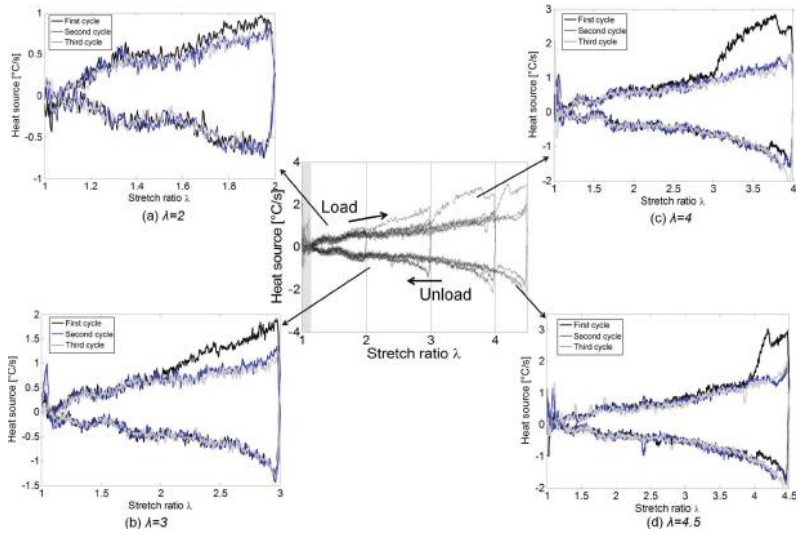

Figure 3. Calorimetrical response obtained with SBR50 for the four maximum stretch ratios tested.

increase in heat source production was observed. Nevertheless, a difference was observed for stretch ratios superior to 3.7: the heat source decreased instead of increasing continuously, before increasing again. Heat continued to be produced (the heat source value remained positive), but at a lower rate. During unloading, the shapes of the heat source profiles absorbed are not similar. In fact, the heat source absorbed at the beginning of the unloading phases decreases with the number of cycles;

Series #4 (three cycles at $\lambda_4 = 4.5$), Figure 3(d): the phenomena are similar to those described above. However, it can be noted that during the first loading, at λ equal to approximately 4, the heat source decreased quasi-instantaneously (by about 0.5°/s), before increasing again. This was previously observed at $\lambda = 3.7$ for the previous maximum stretch ratio applied. This phenomenon seems to depend on the maximum stretch ratio. The understanding of such a phenomenon requires further investigations that were not carried out in this study. For instance, this phenomenon could be explained by the increase in the permanent set between series #3 and series #4.

3.3 *Calorimetric response in filled crystallizable rubbers (NR50)*

For NR50, only the cycles for last two series (λ_3 and λ_4) are presented, due to the fact that a significant permanent set (compared to the maximum stretch ratio applied) was observed for the first two maximum stretch ratios applied. This permanent set induced buckling which disturbed the temperature measurement. Consequently, we have not calculated heat sources for these cycles. It should be noted that, for series #3 and series #4, the maximum stretch ratio applied is superior to that at which crystallization begins. The following comments can be drawn:

Series #3 (five cycles at $\lambda_3 = 4$), Figure 4(a): during the first loading phase, the heat source was positive and increased quasi-linearly with the stretch ratio. The heat source variations for loading and unloading were not symmetrical in a cycle. Such a result cannot be explained only by the effects of entropic coupling and viscosity. Other observations can be made: the heat source produced during the first loading was much larger than that produced during the following four loadings. The heat sources produced during loading were stabilized from the fifth cycle. During unloading, the (negative) heat source profiles seem to be superimposed, meaning that the number of mechanical cycles had no significant effect on the deformation processes during unloading. Moreover, the unloading curve shape shows that the rate of heat source is not constant: a change in the slope sign is observed at a stretch ratio lower than that at which the increase in the heat source was observed during loading. Thus, the highest heat absorption was not obtained at the beginning of the unloading phase. This clearly highlights that the effects of entropic couplings are not preponderant. By comparing the calorimetric responses of unfilled styrene butadiene (Samaca Martinez et al. 2013c) and natural rubbers (Samaca Martinez et al. 2013b), we previously showed that such a response shape is due to stress-induced crystallization. A major difference with SBR50 is the change in the curve shape during the loading phases. Indeed, the heat source was positive and increased quasi-linearly with the stretch ratio, and the following cycles exhibited a sudden increase in the heat

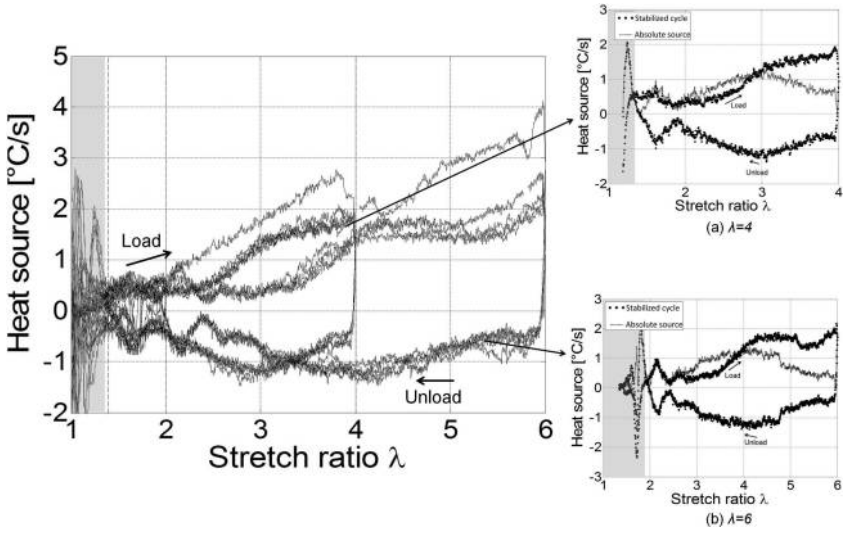

Figure 4. Calorimetrical response obtained with NR50 for the last two maximum stretch ratios tested.

source produced. This could be explained by the fact that mechanical dissipation due to the Mullins effect masks the contribution of stress-induced crystallization during the first cycle. Consequently, the high increase in heat source production could correspond to the occurrence of crystallization.

Series #4 (five cycles at $\lambda_4 = 6$), Figure 4(b): Results were similar to those obtained previously. The only difference is the high increase in the heat source produced after the first loading, which is attributed to stress-induced crystallization and occurs at the highest stretch ratios. This seems to indicate that stress-induced crystallization can be influenced by the Mullins effect. Indeed, a shift is observed in the stretch ratio at which there is a strong increase in the heat source due to crystallization at the second load, if the applied maximum stretch ratio is increased. This increase in heat source production was observed for quite the same nominal stress level. However, this does not prove that stress governs crystallization. In our opinion, it is more probably due to filler network reorganization, which tends to minimize and to homogenize the effects of strain amplification by fillers. Thus, the softened material crystallizes at higher stretch ratio levels, meaning that the crystallinity is lower from the second cycle at a given maximum stretch ratio. This fits well with results recently reported by Zhang et al. (Zhang et al. 2013) and Brüning et al. (Brüning et al. 2012).

3.4 *Calculation of mechanical dissipation corresponding to the Mullins effect*

Classically, the hysteresis loop in terms of the strain-stress relationship is considered to account for mechanical dissipation, so that for instance mechanical dissipation due to viscosity is deduced from the measurement of the hysteresis loop area. In the opinion of the authors, this is not the optimum approach.

Indeed, the hysteresis area is not systematically induced by mechanical dissipation. In unfilled natural rubber, the hysteresis loop is observed only when the material is crystallizing. We have recently shown that in this case, the heat source balance during a cycle shows that no mechanical dissipation is produced (Samaca Martinez et al. 2013b), and consequently the area of the hysteresis loop cannot only be associated with mechanical dissipation. Moreover, the hysteresis loop is not only related to mechanical dissipation but also to thermal dissipation. As the heat source calculated from the heat diffusion equation is not dependent on thermal dissipation, we consider that this is another argument in favour of calculating mechanical dissipation from the calorimetric response. In the present study, the temporal integration of the mechanical dissipation is calculated for each mechanical cycle. This quantity will be still named 'mechanical dissipation' for the sake of simplicity in the following. The calculation of the mechanical dissipation due to Mullins effect is precisely detailed in (Samaca Martinez et al. 2014). Our approach enables us to decouple the contribution of the Mullins effect and the viscosity to the mechanical dissipation. As expected, the Mullins effect is higher between the first and second cycles. The higher the maximum stretch ratio level reached, the higher the mechanical dissipation due to the Mullins effect. At the highest stretch ratios,

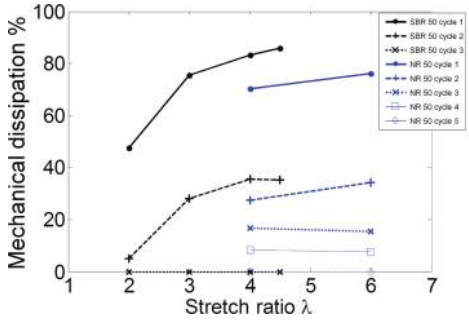

Figure 5. Mechanical dissipation in percent for each cycle versus the maximum applied stretch ratio in filled SBR and NR.

the percentage of mechanical dissipation due to the Mullins effect tends to stabilize.

Figure 5 shows the mechanical dissipation in percent for each cycle versus the maximum applied stretch ratio in both materials. The mechanical dissipation due to the Mullins effect obtained over the second cycle is not negligible in both materials (up to 35% for highest levels). In SBR, the mechanical dissipation due to stress softening is neglected from the third cycle, while we consider that five cycles are necessary in NR. In the case of NR, which is crystallizable under strain, the interpretation must be nuanced by several observations, in particular to define the total mechanical dissipation and consequently what the meaning of the calculation of the mechanical dissipation due to stress softening could be:

- after several cycles at increasing maximum stretch ratios, the first cycle of a higher maximum stretch ratio never undergone before by the material does not join the first monotonous response;
- the calorific activity due to the crystallization/melting process could differ between the first and the following cycles. Typically, the crystallinity maximum is attained at the end of the first loading.

4 CONCLUSION

This study focuses on the calorimetric signature of mechanisms of deformation and damage involved in the stress softening of filled rubbers. More generally, this work is the calorimetric counterpart of "mechanical" studies dealing with the Mullins effect, whose thermomechanical analysis has never been performed before.

Thermal variation was measured by means of infrared thermography and was used to calculate heat sources by using the heat equation. Energy balances performed during each cycle enabled us to identify mechanical dissipation due to viscosity and to mechanisms involved in stress softening. The total mechanical dissipation corresponding to the Mullins effect was calculated for each cycle from the calorimetric response. One of the main results shows that the mechanical dissipation due to the Mullins effect at the second cycle is not negligible for both materials. Moreover, the mechanical dissipation due to the Mullins effect increases less significantly at high stretch ratios, from the second series of cycles in SBR and from the third series of cycles in NR. In NR, stress softening may affect the crystallization process by increasing the stretch ratio at the beginning of the crystallization.

ACKNOWLEDGEMENTS

The authors would like to thank the "Manufacture Française des pneumatiques Michelin" for supporting this study. We also thank D. Berghezan for the fructuous discussions.

REFERENCES

Blanchard A.F. & Parkinson D. 1952. Rubber Chem Technol 52: 799–812.
Bouasse H. & Carrière Z. 1903. *Annales de la faculte des sciences de Toulouse*; 5: 257–283.
Brüning K., Schneider K., Roth S.V. & Heinrich G. 2012. *Macromolecules*; 45: 7914–7919.
Bueche F. J Appl Polym Sci 1960; 4: 107–114.
Chrysochoos A. 1995. *In: Colloque photomécanique;* 201–211.
Diani J., Brieu M. & Gilormini P. 2006. *Int J Solids Struct*; 43: 3044–3056.
Hamed G.R. & Hatfield S. 1989. *Rubber Chem Technol*: 143–156.
Houwink R. 1956. *Rubber Chem Technol*; 29: 888–893.
Klüppel M. & Schramm M. 2000. *Macromol Theor Simulat*; 9: 742–754.
Kraus G., Childers C. & Rollman K. 1966. *J Appl Polym Sci*; 10: 229–240.
Marckmann G., Verron E., Gornet L., Chagnon G., Charrier P. & Fort P. 2002. *J Mech Phys Solids*; 50: 2011–2028.
Mullins L. 1948. *Rubber Chem Technol*; 21: 281–300.
Samaca Martinez J.R., Le Cam J.-B., Balandraud X., Toussaint E. & Caillard J. 2013a. *Polymer* 54: 2717–2726.
Samaca Martinez J.R., Le Cam J.-B., Balandraud X., Toussaint E. & Caillard J. 2013b. *Polymer* 54: 2727–2736.
Samaca Martinez J.R., Le Cam J.-B., Balandraud X., Toussaint, E. & Caillard, J. 2013c. *Polym Test* 32: 835–841.
Samaca Martinez J.R., Le Cam J.B., Balandraud X., Toussaint, E. & Caillard, J. 2014. *Eur Polym J* 55: 98–107.
Zhang H., Scholz A.K., Merckel Y., Brieu M., Berghezan D., Kramer E.J., et al. 2013. J Polym Sci; 51: 1125–38.